Bio-Inspired Flower Robot for Emotional Human-Robot Interaction

Qingyue Liu, Guojie Xu, Canrui Yang, Xunsheng Du, Igarashi Go, and Hongqiang Wang

***Abstract*—Mental health problems are common worldwide, but the available support systems and healthcare services are insufficient and inadequate. Social robots offer a promising solution to achieve social interaction and emotional connection. Nature-inspired architectural robotics can seamlessly blend into human daily life by reshaping future living environments. In this work, inspired by natural flowers, we designed a flower robot with a realistic morphology that simulates the opening-closing, rhythmic movements, and stem-bending movement. Building on the morphological design, we integrated a flex sensor into the petals to enable touch-induced tactile feedback, mimicking the touch-induced plant-like seismonastic movement. Furthermore, we incorporated voice interaction powered by a local large language model (LLM) to achieve adaptive intent understanding and personalized semantic engagement, thereby enhancing interaction flexibility compared to the repetitive tasks and rigid protocols of traditional social robots. Finally, the human-robot interaction (HRI) experiment demonstrated that the flower robot significantly reduced participants' negative emotions and provided positive social engagement. This work developed a bio-inspired flower robot, offering a promising pathway to social interaction and soothing presence.**

***Index Terms*—Bio-inspired robot, soft robots, social robots, flower robot, human-robot interaction.**

Received 8 November 2025; accepted 4 April 2026. Date of publication 22 April 2026; date of current version 4 May 2026. This article was recommended for publication by Associate Editor X. Zhang and Editor A. Peer upon evaluation of the reviewers' comments. This work was supported in part by the Natural Science Foundation of China under Grant 52275021 and Grant 52450323, in part by the Natural Science Foundation of Guangdong Province of China under Grant 2024A1515010183, in part by 2025 Shenzhen-Hong Kong-Macau Science and Technology Program (Category C) under Grant SGCX20250526153900001, in part by Guangdong Provincial Research Support Program under Grant 2019QN01Z733, and in part by the SUSTech Undergraduate Innovation and Entrepreneurship Training Program under Grant S202514325008. *(Qingyue Liu and Guojie Xu contributed equally to this work.) (Corresponding author: Hongqiang Wang.)*

This work involved human subjects or animals in its research. Approval of all ethical and experimental procedures and protocols was granted by the Southern University of Science and Technology Science Ethics Committee under Application No. 2025PES399, and performed in line with the Declaration of Helsinki.

Qingyue Liu, Guojie Xu, and Canrui Yang are with the SUSTech Institute of Robotics Research, Southern University of Science and Technology, Shenzhen 518055, China.

Xunsheng Du and Igarashi Go are with Sony, Unit 1, Shenzhen 518031, China.

Hongqiang Wang is with the SUSTech Institute of Robotics Research, Department of Mechanical and Energy Engineering and Guangdong Provincial Key Laboratory of Human-Augmentation and Rehabilitation Robotics in Universities, Shenzhen 518055, China, and also with the Southern University of Science and Technology, Shenzhen 51855, China (e-mail: wanghq6@sustech.edu.cn).

This article has supplementary downloadable material available at https://doi.org/10.1109/LRA.2026.3686643, provided by the authors.

Digital Object Identifier 10.1109/LRA.2026.3686643

I. Introduction

Mental health is a crucial aspect of overall well-being, and mental health problems are common all over the world. In 2020, rates of common mental health disorders like depression and anxiety rose by more than 25% [1]. The need for mental health is urgent, but responses are insufficient and inadequate. Traditional treatments for mental health problems vary, but they often consume significant time, resources, and manpower, and place tremendous pressure on families and caregivers [2].

Robotics-based interventions, particularly socially assistive robotics, offer a promising solution to bolster support for both homes and caregivers, ultimately enhancing personalized therapeutic assistance [3]. The social robot is regarded as "an autonomous or semi-autonomous robot that interacts and communicates with humans by following the behavioral norms expected by the people with whom the robot is intended to interact" [4]. Among social robots, copresent robots [5] are especially promising due to their physical embodiment and shared interactive space, which enrich nonverbal communication and foster more authentic social dynamics, with important implications for HRI [6]. Within this category, nature-inspired architectural robotics can seamlessly blend into human daily life by reshaping future living environments, presenting an interactive and intelligent physical environment [7]. Flowers, ubiquitous in daily life and admired for symbolic meaning, have inspired numerous works of art and literature due to their exquisite form [8]. Several studies have reported that flowers may help reduce stress levels [9], have a restorative effect on attention, and improve cognitive performance [10], [11]. Furthermore, gardening activities, such as flower viewing, may alleviate symptoms of depression and enhance overall mental well-being [12]. Drawing on these findings, flowers can be regarded as a unique medium for social interaction. However, there is limited research on social robots utilizing flowers as carriers.

In the field of robotics, flower-inspired robots have attracted increasing attention. H. K. Park et al. designed a flower robot actuated by tendon mechanisms and micro-electro-mechanical systems, which enabled partial control of the flower, stem, and leaves [13]. Later, Truong-Thinh et al. introduced a spring-tendon hybrid mechanism to improve motion smoothness [14]. These early studies provided the foundation for integrating flower-inspired robots. However, the exposed motor-tendon transmission and rigid components not only disrupt the visual integrity of the natural flower-like appearance, but also pose collision risks during human-robot interaction (HRI). The emergence of soft robots has introduced a new paradigm for HRI safety. Min-Woo Han et al. introduced a novel soft morphing structure inspired by blooming flowers [15]. It uses loop-linked knitted materials to enable dynamic shape changes in response to external stimuli, mimicking the opening and closing of flowers. Castillo Ugalde et al. proposed a pneumatic actuation approach, employing inflatable membranes and silicone petals to create a fully soft robotic flower. This design successfully overcame the limitations of rigid structures and achieved both morphological and functional biomimicry [16]. However, there are still several noticeable gaps when compared to the desired flower-like social robot: (1) Appearance and aesthetics: when uninflated, the petals lie flat in a 2D plane. Upon inflation, the large inter-petal gaps lacks the natural layering and overlapping of real flowers, leading to a distinct morphological difference. The robot's similarity to natural organisms can evoke users' biophilic tendencies, reducing unfamiliarity and shortening the adaptation period during HRI [17]. (2) Interactive features: the interaction relies on predefined protocols, which, over time, can lead to reduced user engagement and diminished long-term motivation for interaction.

A desired flower-like social robot should possess the following characteristics: (1) The core feature should be an appearance that captures the beauty of a real flower. This trait enhances users' willingness to interact with the robot, fostering emotional engagement and building rapport. (2) It should have tactile interaction capabilities, allowing users to touch the flower and receive corresponding responses, thus enhancing emotional engagement [18]. (3) The interaction mode should shift from repetitive templates to a more adaptive, and intelligent interaction paradigm [19].

In this work, inspired by the expansion and deformation of petal base cells of natural flowers [20], [21], we designed a flower robot with a realistic morphology that simulates the opening-closing and rhythmic movements of flowers, as well as the bending movement of the flower stem (Fig. 1). Building on this morphological design, we attached a flex sensor to the petals, which allows tactile feedback and mimics the touch-induced plant-like seismonastic movement. To further enhance the interaction, we also introduced the voice interaction powered by a local large language model (LLM) to provide personalized and intelligent interactions, maintaining freshness and overcoming the boredom caused by repetitive tasks in traditional social robot interactions. Finally, the HRI experiment demonstrated that the flower robot can provide people with emotional recognition and interaction.

In this article, Section II describes the design of the flower robot, including the flower part and the stem part. Section III describes the system integration and demonstration of the flower robot. Section IV implements a HRI experiment and investigates the social functions of the flower robot. Finally, Section V concludes the article by highlighting the effectiveness of the proposed design in creating a flower robot with a realistic form and social value.

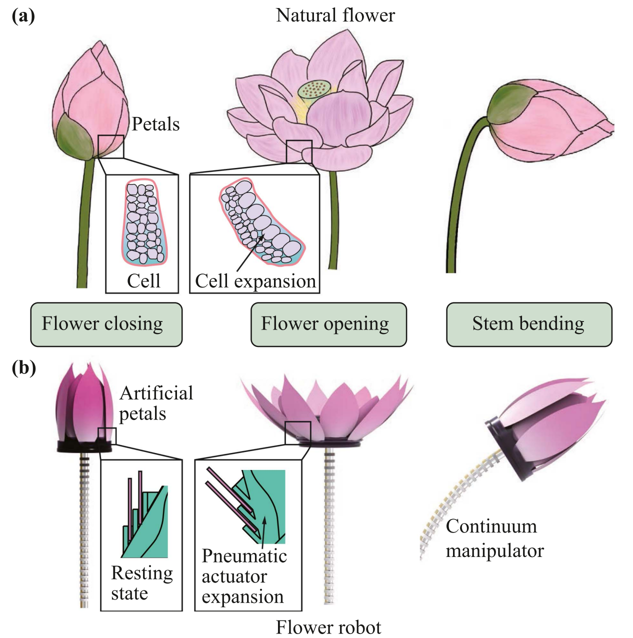

Fig. 1. The flower robot and its working principle. (a) Natural flowers closing, opening, and stem bending. (b) Flower robot closing, opening, and stem bending.

II. Design of the Flower Robot

A. Inflation Behavior of Elastomeric Conical Shells for Pneumatic Actuators

Natural flower opening mainly results from the uneven expansion of cells at the petal base and the inner and outer epidermal cells, which causes the petals to bend and unfold [20], [21]. Inspired by the expansion deformation of petal base cells, we designed a pneumatic actuator to simulate the deformation of basal cells to open and close the flower. The pneumatic actuator should meet the following design requirements: during the inflation process of the pneumatic actuator, the petal bonding region (barb-like joint) is required to undergo a directional change of a relatively large angle to realize petal bending, while radial expansion at this region should be minimized to prevent interference between adjacent petals during closure.

Among different schemes, a thin-walled conical pneumatic actuator is more suitable for maintaining the petals in a closed posture when uninflated, while enabling bending at the petal base upon inflation. In the initial design, the sidewalls were designed to have a uniform wall thickness (Fig. 2(a)). The bottom diameter was chosen to match the size of natural counterparts (such as lotus and tulip).

A finite element model was built to simulate the expansion deformation of the pneumatic actuator. The sidewall material (Ecoflex 00-50, Smooth-On) is considered hyperelastic, and the hyperelastic model used is the Yeoh model with parameters $C_1 = 0.019$, $C_2 = 0.0009$, and $C_3 = 4.25 \times 10^{-6}$ MPa [22]. The top and bottom base materials (Dragon Skin 10, Smooth-On) are also considered hyperelastic, and modeled with the Neo-Hookean model, where $C_1 = 0.0425$ MPa [22]. Fixed

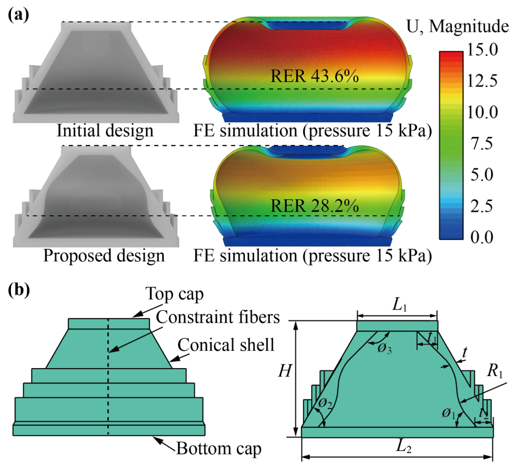

Fig. 2. Comparison of the initial design and the proposed design during expansion with a 15 kPa pressure. (a) Structural design and finite element modeling of pneumatic actuators. (b) Structural parameters of pneumatic actuators.

constraints on the upper and lower surfaces were applied to simulate the three fibers that limit the actuator's axial expansion. The pneumatic actuator was subjected to internal pressure loads at various levels. The finite element simulation was performed using Abaqus 2021.

Through finite element analysis, it was found that under the initial design configuration, the radial expansion rate (RER), defined as RER $= \frac{L-L_0}{L_0} \times 100\%$, at the second-layer petal bonding region was as high as 43.6% (where L_0 represents the original diameter and L is the inflated diameter). To meet the desired requirements mentioned before, an optimized design with a non-uniform thickness and an S-shaped contour was proposed, providing a gradual transition between different wall sections. The finite element analysis showed that under this optimized configuration, the RER decreased to 28.2% at the same position, representing a reduction of approximately 35%. The structural parameters before and after the design optimization are as follows: while the height ($H = 28$ mm) and cap diameters ($L_1 = 19.44$ mm, $L_2 = 46$ mm) remain unchanged, the proposed design adopts a non-uniform profile to suppress radial expansion. Specifically, the waist thickness (t) was increased from 1.5 mm to 2.1 mm, supplemented by a shoulder thickness ($t_1 = 5.5$ mm), a bottom thickness ($t_2 = 4.5$ mm), and a waist radius ($R_1 = 10$ mm). Additionally, while the cone bottom angle (α_2) is fixed at 60°, the inner chamber top angle (α_1) was reduced to 50° and the bottom angle (α_3) was increased from 120° to 135°.

B. Experimental and Finite Element Analysis of Pneumatic Actuator

Finite element analyses and experiments of the pneumatic actuator were conducted across a range of air pressures. The results demonstrated that the actuator's deformation increased in response to higher air pressure. At 15 kPa, the actuator deformation essentially meets the design requirements. This provides a reference for subsequent closed-loop air pressure control of

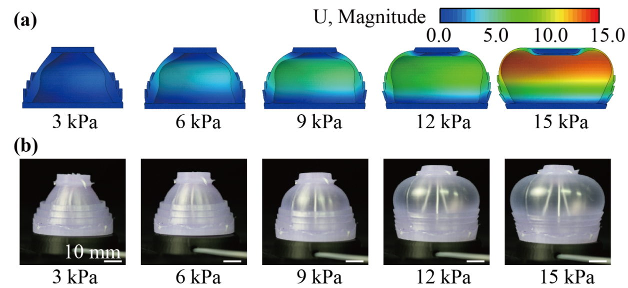

Fig. 3. Experimental and finite element snapshots of the pneumatic actuator during inflation at different air pressure levels. (a) Finite element simulation of pneumatic actuators at 3 kPa–15 kPa. (b) Experimental of pneumatic actuators at 3 kPa–15 kPa.

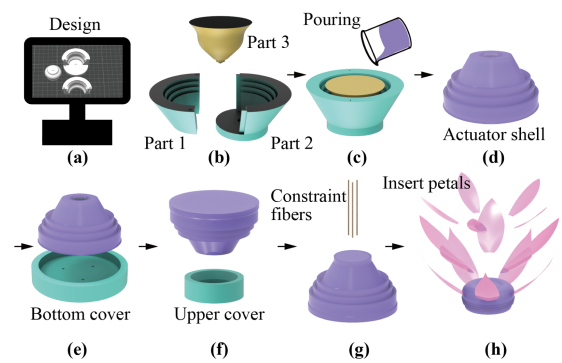

Fig. 4. The fabrication process of the pneumatic actuator. (a) The mold design for pneumatic actuators. (b) The mold was fabricated and assembled. (c) The liquid silicone was poured into it for molding. (d) The pneumatic actuator shell. (e) Casting the bottom cover. (f) Casting the upper cover. (g) The constraint fibers were attached along the z-axis. (h) The artificial petals were affixed to the outer surface of the actuator.

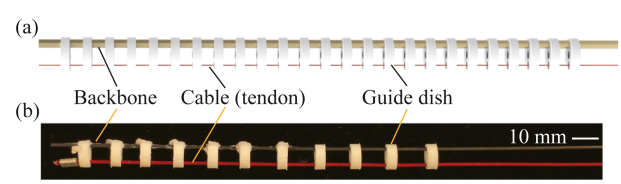

Fig. 5. The tendon-driven continuum manipulator. (a) Design of the tendon-driven continuum manipulator. (b) Prototype of the tendon-driven continuum manipulator.

the actuator. The simulation and experimental results show a consistent radial expansion deformation, while the experimental results show a greater axial expansion than the simulation results. This is due to the elastic deformation of the constraint fibers (Fig. 3) .

C. Fabrication Process of Pneumatic Actuator

To fabricate the pneumatic actuator, we first designed a corresponding mold for casting. Specifically, the mold was fabricated using a 3D printer, and then liquid silicone (Ecoflex 00-50,Smooth-On) was poured into it to form the actuator shell. After the silicone was fully cured, the shell was carefully removed from the mold and subsequently sealed with top and

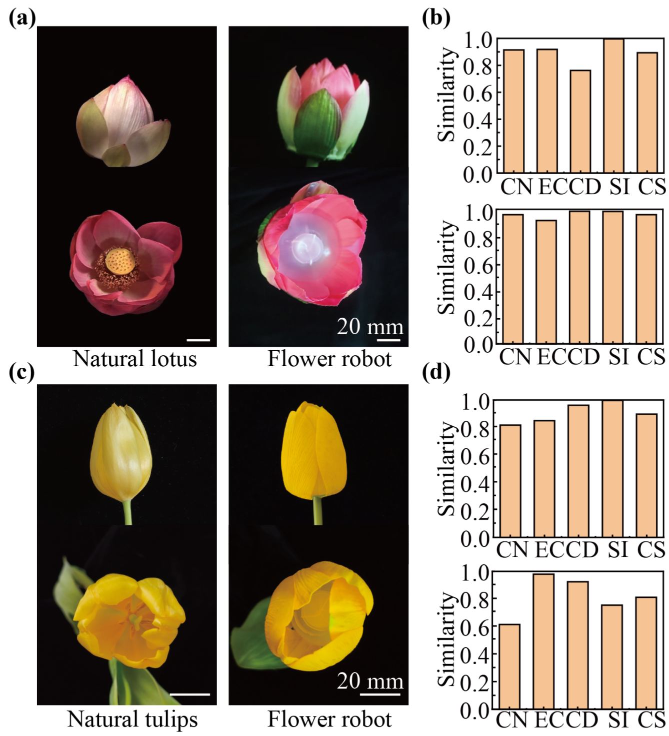

Fig. 6. The comparison of contour similarity between the flower robot and the natural flower. (a) Natural lotus (from https://linktr.ee/WyvernFilms, without needing permission) and flower robot (lotus). (b) Comparison of related indicators. (c) Natural tulips and the flower robot (tulips). (d) Comparison of related indicators.

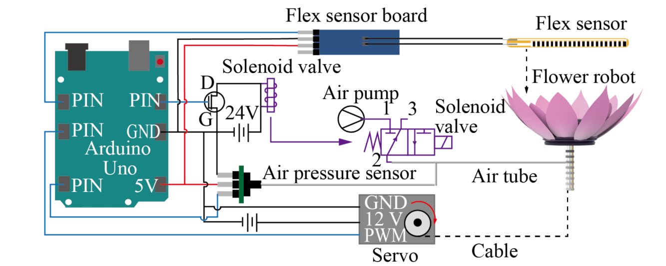

Fig. 7. Overall system logic of the flower robot, showing the coordination of the pneumatic actuation, electrical control, and servo mechanisms.

bottom covers made from silicone (Dragon Skin 10, Smooth-On). To prevent undesired deformation during inflation, constraint fibers (diameter 0.5 mm, steel wire) were attached along the z-axis so as to limit vertical expansion. Finally, the complete flower-like structure was assembled by affixing artificial petals into pre-designed grooves on the actuator's outer surface using a silicone-specific adhesive (5562 Instant Adhesive, Kai Bing Tuan), as illustrated in Fig. 4.

D. Design of a Tendon-Driven Continuum Manipulator

A tendon-driven continuum manipulator was designed to realize the bending movement of the flower stem (Fig. 5). The tendon-driven continuum manipulator consists of a backbone (diameter 1.2 mm, Nitinol wire), cable (diameter 1.0 mm, steel wire), and guide dish (3D printing, polylactic acid (PLA)). The continuum manipulator is actuated by one tendon routed along its backbone.

III. System Integration and Demonstration of the Flower Robot

A. The Contour Similarity Between the Designed Flower Robot and Its Natural Counterpart.

The flower robot replicates the opening process of a real flower. We compared the morphological similarity between flower robots and their natural counterparts (lotus and tulip) in both closed and opening states (Fig. 6). Specifically, top-view images were captured for the opening state of natural and robotic lotuses, while front-view images were taken for their closed states.

An image edge detection algorithm was then applied to extract floral contours. Quantitative comparisons were performed using five metrics: contour naturalness (CN), edge complexity (EC), shape irregularity (SI), curvature distribution (CD), and comprehensive similarity (CS). Experimental results demonstrated that the comprehensive similarity between natural and robotic lotuses exceeded 90%. To demonstrate the broad applicability of our design strategy, a tulip-inspired soft robot was designed and fabricated. A morphological comparison with its natural counterpart revealed a comprehensive similarity of over 85%.

B. Air Pressure Control System

The basic control logic of the flower robot is shown in Fig. 7. The hardware system consists of an Arduino Uno, a MOSFET, a solenoid valve, a pressure sensor, a pneumatic pump, and several DuPont wires. After being powered, the pump delivers air into the actuator chamber through the valve controlled by the MOSFET. When the pressure sensor detects that the pressure has exceeded the upper limit, the Arduino is programmed to close the valve. It will reopen only after the pressure drops to a lower threshold. The pneumatic system is driven by the D23L-22 Brushless DC Air Pump, chosen for its low-noise operation (< 43 dB) at the expense of a modest flow rate of 0.95 L/min, which takes 18–21 seconds for the flower to open fully.

C. Tactile Interaction and Voice Interaction Based on Large Language Models System

Fig. 8 shows the logic of the HRI system, which includes two parallel input pathways: tactile interaction and voice-emotional interaction. For tactile interaction, a flex sensor (flex sensor 2.2) is attached and hidden inside the outer petals to detect changes in bending angle, and minimize the impact on the overall beauty of the flower (Fig. 9). During the tactile interaction (Fig. 10), the flower robot is initially in the opening state. When a user touches a petal and the flex sensor detects an angle change greater than the predefined threshold (25°), the tactile control logic is activated, causing the flower robot to close (pneumatic chamber deflation) and the stem to bend, mimicking the plant-like seismonastic movement.

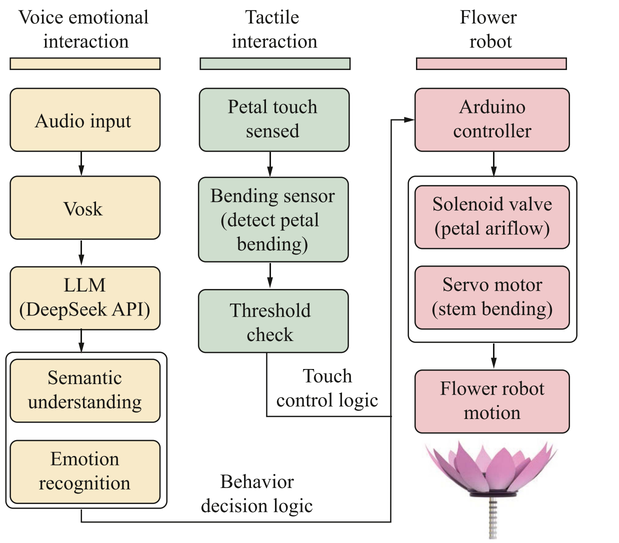

Fig. 8. Diagram of software components. Two parallel pathways are implemented: (i) voice–emotional interaction, where Vosk and a local LLM analyze speech and generate actuator commands; and (ii) tactile interaction, where a flex sensor detects petal deformation beyond a threshold, triggering chamber deflation and stem bending.

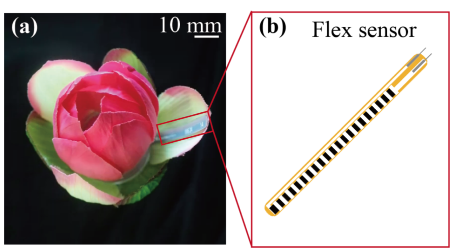

Fig. 9. Integration of flex sensor and flower robot. (a) The flex sensor is integrated into the inner surface of the petals. (b) Enlarged view of the flex sensor.

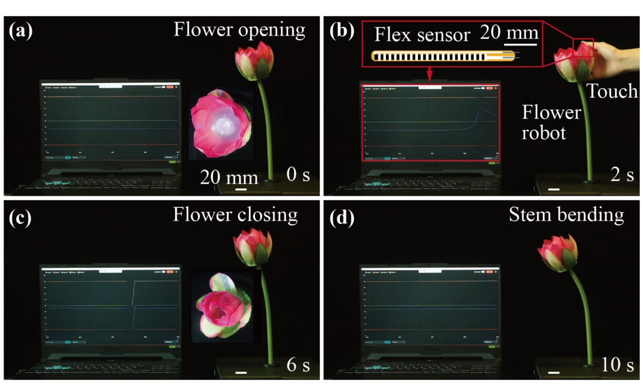

Fig. 10. The tactile interaction demonstration of the flower robot. (a) The flower robot remains open in its initial state. (b) When a user touches a petal. (c) The flower robot closes. (d) The stem bends.

As shown in Fig. 11, users express their emotions with the flower robot through voice interaction. The existence of a LLM enables an adaptive system with semantic perception capability to understand the user's unstructured natural language inputs. Once the program starts, Vosk (a speech recognition tool) converts spoken input into text. This text is then passed to a local LLM, where an AI agent analyzes both the semantics and the emotional tone of the input. Based on this analysis, the agent determines the appropriate command, which is sent to the Arduino for execution. The resulting movements of the flower robot are then presented to the user as feedback. We utilized DeepSeek-V3 and implemented the raw prompting strategy involving writing Python code ourselves to interact with the LLM. The model was accessed via the standard 'deepseek-chat' API endpoint, which provided the most current stable release of the V3 architecture during our experimental period (late 2025). Table II showed some typical detectable states/intents and the corresponding repertoire of robot behaviors.

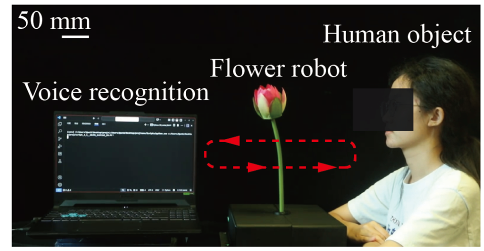

Fig. 11. The voice–emotional interaction demonstration of the flower robot.

TABLE I
INTERACTIVE PROMPTS ON THE SCREEN USED IN THE EXPERIMENT

No.	Interaction Prompts (English Translation)
1	Could you tell me about something that has been bothering or stressing you out lately?
2	Why does this bother you? Or how does this affect you?
3	Now you can touch my petals and let me feel your emotions.
4	In moments like this, what usually helps you feel a little better?
5	If I were a little flower who could listen, what would you want me to say to comfort you right now?
6	I can feel your emotions. Let's do a breathing exercise to relax. Say to me, "I am ready for deep breathing," then follow my petals and we will begin.
7	Now, please think of a small thing that has warmed your heart lately. At that moment, what did you feel?
8	If that feeling of joy had a color, what do you think it would look like?
9	If you were to share that warmth with others, what way would you choose?
10	Please gently close your eyes, imagine a beam of gentle light shining on you, breathe slowly, and relax gradually.

IV. Human-Robot Interaction Experiment

A. Experiment Setup

Our experiment aims to answer the following questions: (1) How do users perceive the social attributes of the flower robot? (2) How will the flower robot affect users' emotions after interaction? Based on our design intention, which relieves mental health issues and promotes emotional interaction, we posit the following hypotheses: (1) The bio-inspired flower robot will be perceived as highly safe and likeable by users. (2) The flower robot will significantly reduce users' negative emotions while promoting positive emotions.

TABLE II
SOME DETECTABLE STATES/INTENTS AND THE CORRESPONDING REPERTOIRE OF ROBOT BEHAVIORS

Input Utterance	LLM Classification		Reasoning	Robot Motion	
	Emotion	Semantic		Flower	Stem
"I got first place in the competition!"	Positive	Unknown	High positive valence and explicit achievement trigger the robot's active state to celebrate with the user.	Open	\
"I stayed up late working on this project."	Negative	Unknown	Expressions of fatigue and overwork default the system to a rest or supportive state to encourage relaxation.	Close	Bend
"My best color is blue like the sky."	Neutral	Unknown	A purely declarative narrative statement with no active intent or emotional trigger to act upon.	Breathe	\
"Time to say goodbye, see you later."	Neutral	OFF	The explicit termination initiates closing sequence.	Close	Bend

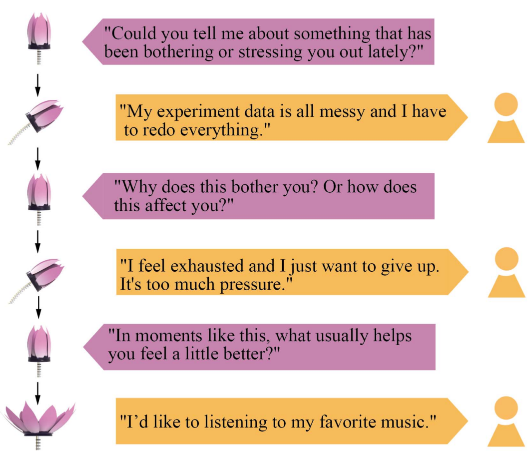

Fig. 12. An illustrative interaction sequence showing the interaction progress. Left icons represent the flower robot's physical morphology status, while right icons represent the user. Purple bubbles represent pre-set prompts displayed on the screen, while orange bubbles represent the user's verbal responses.

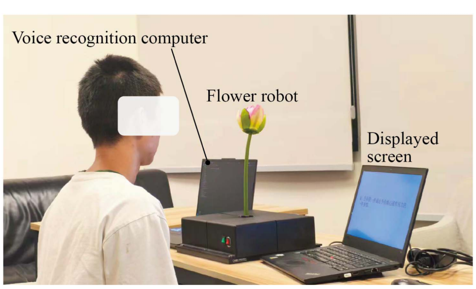

Fig. 13. The environmental setup conditions. From left to right are the voice recognition computer, the flower robot, and a display screen.

We configured an independent room as the experimental venue. A table was placed in the center of the room, on which the experimenter's computer and the flower robot were positioned (from left to right). Participants were seated in front of the robot. A display screen was set to assist the experiment (Fig. 13). A pilot study was conducted with 4 participants (Mean age = 24.5, standard deviation (SD) = 6.45) to validate that the experimental setup could effectively elicit emotional responses. Improvements include prolonging the duration between questions displayed on the screen (from 20 s to 30 s) and revising confusing prompts. The research protocol was approved by the ethics committee of the research institute with the approval number 20250399. Before the experiment, each participant signed an informed consent. In the formal study, 20 participants (Mean age = 23.05, SD = 3.23; 17males and 3 females) were recruited. All participants are from China, and the language of interaction, such as the caption displayed, is set to be Chinese to ensure a comfortable interaction environment and accurate results. Besides, no participants reported pre-existing mental health conditions or clinically significant stress issues before attending the experiment. Fig. 12 shows a desired interaction log.

We employed the Positive and Negative Affect Schedule (PANAS) [23] to assess the participants' emotional engagement, and the Godspeed Questionnaire (GQS) [24] to assess the robot's perceived usefulness. Additionally, we designed a subjective questionnaire to collect participants' opinions on the strengths and improvements of the flower robot. The entire procedure lasted 20 to 30 minutes and consisted of five phases: (1) Introduction: researchers introduce the purpose and procedure of the experiment and ask participants to sign the informed consent. After that, they are required to finish the PANAS to record their emotions at that time. (2) Familiarization: researchers exhibit a basic function of the system by guiding participants to finish several simple interactions with the robot. (3) Formal task: participants are required to have a 5-minute communication with the robot, which should be centered on a specific experience or emotion. In case they do not know what to communicate with the robot, researchers set a series of questions on the display screen to assist the interaction (Table I). (4) Questionnaire completion and feedback: after the whole experiment, participants finished another set of questionnaires compromised of another PANAS, a GQS and several subjective Questions: Q1: how did you feel about your overall interaction with the flower robot? Was there a particular moment that stood out to you? Q2: do you find the flower robot useful? If so, in what way do you think it was most useful? Q3: if you were to improve the flower robot, what feature would you most like to change or add?

B. Results

There are 20 participants in total involved in and finished our experiment, whose statistics are taken into consideration in the last result. For the effect of emotional engagement, we examined

TABLE III
THEMATIC ANALYSIS OF USER FEEDBACK FROM SUBJECTIVE QUESTIONNAIRE (N=20)

Sentiment	Key Theme	Count	Representative Quote[1]
Positive (N=14)	Emotional Resonance	5	"Following the breathing felt special, like a shared breath."
	Lifelike Animacy	5	"The flower reacted to my expressions... seemed to have vitality."
	Visual Novelty	4	"Felt quite novel, especially during the deep breathing phase."
Neutral (N=3)	Functional / Okay	3	"It was okay. It moved when asked and stopped when asked."
Negative (N=3)	Mechanical Limits	2	"The motion was a bit slow."
	Intelligence Limits	1	"Fun, but it didn't seem to understand human speech very well."

[1]Original responses were in Chinese and translated by the authors.

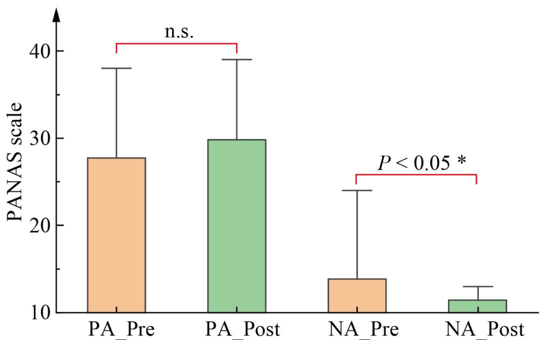

Fig. 14. Participants' questionnaire ratings on a 1–5 scale using the PANAS. PA_Pre: positive affect (pre-test). PA_Post: positive affect (post-test). NA_Pre: negative affect (pre-test). NA_Post: negative affect (post-test). n.s.: not significant. $P < 0.05^{*}$: significant. Error bars indicate standard error (SE).

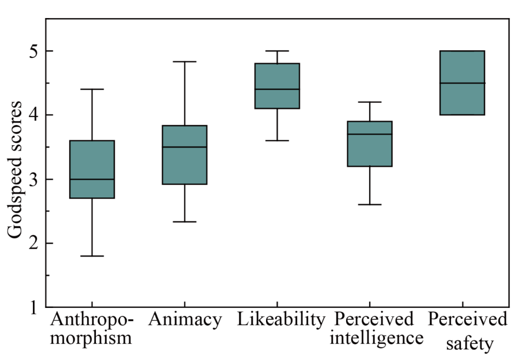

Fig. 15. Participants' questionnaire ratings on a scale of 1–5 using the GQS.

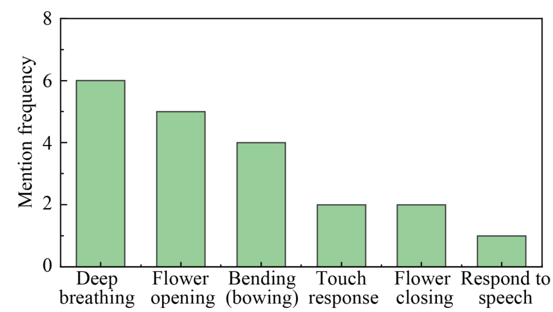

Fig. 16. Participants' questionnaire on the most memorable moments.

the paired sample t-test for PA (positive affect) and NA (negative affect) sections before and after the interaction (Fig. 14).

For NA, the result showed a statistically significant decrease after the interaction ($t(19) = 3.84, p = 0.001$), with a medium effect size (Cohen's $d = 0.56$). For PA, although there was an increase in the mean score, the difference was not statistically significant ($t(19) = -1.75, p = 0.097, d = 0.33$).

Regarding the robot's perception, the GQS results (Fig. 15) indicated that Perceived Safety received the highest score (Mean = 4.429, SD = 0.455), followed by Likeability (Mean = 4.333, SD = 0.530). Anthropomorphism received a moderate score (Mean = 2.964, SD = 0.834).

For the qualitative feedback, we manually code the responses to identify dominant sentiments (Positive, Neutral, Negative). Responses containing explicit praise or expressions of relaxation were categorized as Positive, while those focusing on technical limitations were categorized as Negative. Details are showed in Table III. As for the impressive moments (Fig. 16), most participants mentioned the "deep breathing" (6 mentions). Other common themes included "flowers blooming" (5 mentions), "flowers bending" (4 mentions), and "touch perception" (2 mentions).

C. Discussion

The results showed that the change in participants' negative emotion scores reached a highly statistically significant level. This directly supports our hypothesis that the flower robot effectively mitigates negative emotions, and is consistent with the frequent use of descriptions such as "relaxing" (2 times) and "calming" (3 times) in user subjective feedback. However, although the average score showed an increase in positive emotions, the change was not statistically significant, which showed a limited effect against our hypothesis that the flower robot promoted positive emotions. We assume this is because participants have already been in a relatively positive emotional state at baseline (Mean= 27.75 out of 50). Future studies with a more diverse participant pool are considered to reveal the robot's potential to further enhance positive emotions.

Regarding the robot's perception, although Anthropomorphism doesn't receive a high score, its emotional paradigm and perceptual intelligence are still applicable to the flower robot. The results of Perceived Safety and Likeability also indicate that participants held a positive emotional attitude toward the flower robot, feeling comfortable and unthreatened during the interaction. This is consistent with our second hypothesis.

The main limitations of our flower robot prototype include a lack of fast response, the omission of other multi-modal outputs such as visual or voice output, a skewed participant demographic (17 males and 3 females), and the controlled laboratory context of our initial study. In the future, we will explore multi-modal outputs, including expressive voice, variable lighting, and music. Subsequent user studies will be carried out in more natural environments with larger, more diverse samples—specifically aiming for a balanced gender ratio (e.g., 1:1) to thoroughly assess the system's real-world applicability and long-term engagement potential.

V. Conclusion

This work presents a bio-inspired flower robot, offering a promising pathway to social interactions and emotional connections. Firstly, its realistic morphology simulates the opening-closing and rhythmic movements of petals, along with stem bending. Secondly, the integration of a flex sensor on the petals enables tactile feedback, replicating the touch-induced responses observed in plant-like seismonastic movement. Thirdly, by incorporating voice interaction powered by a local LLM, the system offers personalized and intelligent interactions, thereby maintaining user engagement and overcoming the repetitiveness that often plagues traditional social robot interactions. Finally, the HRI experiment demonstrated that the flower robot decreased participants' negative emotions to a highly statistically significant level. Likeability and perceived safety received the highest score, indicating that participants held a positive emotional attitude toward the flower robot.

References

[1] World Health Organization, "World mental health report: Transforming mental health for all," Geneva, Switzerland, 2022. [Online]. Available: https://www.who.int/publications/i/item/9789240049338

[2] V. H. Mackintosh, R. P. Goin-Kochel, and B. J. Myers, "What do you like/dislike about the treatments you're currently using? A qualitative study of parents of children with autism spectrum disorders," *Focus Autism Other Devlop. Disabilities*, vol. 27, no. 1, pp. 51–60, 2012.

[3] B. Scassellati, "How social robots will help us to diagnose, treat, and understand autism," in *Proc. Robot. Res.: Results 12th Int. Symp.*, 2007, pp. 552–563.

[4] C. Bartneck and J. Forlizzi, "A design-centred framework for social human-robot interaction," in *Proc. RO-MAN 2004. 13th IEEE Int. Workshop Robot Hum. Interactive*, 2004, pp. 591–594.

[5] J. Li, "The benefit of being physically present: A survey of experimental works comparing copresent robots, telepresent robots and virtual agents," *Int. J. Hum.- Comput. Stud.*, vol. 77, pp. 23–37, 2015.

[6] J. Wainer, D. J. Feil-Seifer, D. A. Shell, and M. J. Mataric, "The role of physical embodiment in human-robot interaction," in *Proc. ROMAN 2006-The 15th IEEE Int. Symp. Robot Hum. Interactive Commun.*, 2006, pp. 117–122.

[7] K. E. Green, *Architectural Robotics: Ecosystems of Bits, Bytes, and Biology*. Cambridge, MA, USA: MIT Press, 2016.

[8] B. Seaton, *The Language of Flowers: A History*. Charlottesville, VA, USA: Univ. of Virginia Press, 2012.

[9] T. Bringslimark, T. Hartig, and G. G. Patil, "The psychological benefits of indoor plants: A critical review of the experimental literature," *J. Environ. Psychol.*, vol. 29, no. 4, pp. 422–433, 2009.

[10] R. K. Raanaas, K. H. Evensen, D. Rich, G. Sjøstrøm, and G. Patil, "Benefits of indoor plants on attention capacity in an office setting," *J. Environ. Psychol.*, vol. 31, no. 1, pp. 99–105, 2011.

[11] B. Grinde and G. G. Patil, "Biophilia: Does visual contact with nature impact on health and well-being?," *Int. J. Environ. Res. Public Health*, vol. 6, no. 9, pp. 2332–2343, 2009.

[12] M. T. Gonzalez, T. Hartig, G. G. Patil, E. W. Martinsen, and M. Kirkevold, "Therapeutic horticulture in clinical depression: A prospective study of active components," *J. Adv. Nurs.*, vol. 66, no. 9, pp. 2002–2013, 2010.

[13] H. L. Huang, S.-H. Park, J.-O. Park, and C.-H. Yun, "Development of stem structure for flower robot using SMA actuators," in *Proc. IEEE Int. Conf. Robot. Biomimetics*, 2007, pp. 1580–1585.

[14] N. Truong-Thinh and N. Ngoc-Phuong, "Design and development of continuum structure for robotic flower," in *Proc. IEEE Int. Conf. Robot. Biomimetics*, 2011, pp. 118–123.

[15] M.-W. Han and S.-H. Ahn, "Blooming knit flowers: Loop-linked soft morphing structures for soft robotics," *Adv. Mater.*, vol. 29, no. 13, 2017, Art. no. 1606580.

[16] A. C. Ugalde, S. L. Zhiyu, C. C. Camara, W. Yixiao, and P. V. Y. Alvarado, "Nature's Embrace: Development and validation of a pneumatic soft robotic flower for calming interactions," in *Proc. IEEE 7th Int. Conf. Soft Robot.*, 2024, pp. 601–608.

[17] M. B. Christiansen, A. Rafsanjani, and J. Jørgensen, "It brings the good vibes: Exploring biomorphic aesthetics in the design of soft personal robots," *Int. J. Social Robot.*, vol. 16, no. 5, pp. 835–855, 2024.

[18] T. Olugbade, L. He, P. Maiolino, D. Heylen, and N. Bianchi-Berthouze, "Touch technology in affective human–, robot–, and virtual–human interactions: A survey," *Proc. IEEE*, vol. 111, no. 10, pp. 1333–1354, Oct. 2023.

[19] B. Scassellati et al., "Improving social skills in children with ASD using a long-term, in-home social robot," *Sci. Robot.*, vol. 3, no. 21, 2018, Art. no. eaat7544.

[20] M. Ke, Z. Gao, J. Chen, Y. Qiu, L. Zhang, and X. Chen, "Auxin controls circadian flower opening and closure in the waterlily," *BMC Plant Biol.*, vol. 18, no. 1, 2018, Art. no. 143.

[21] H. Zhang et al., "The mechanism underlying asymmetric bending of lateral petals in delphinium (ranunculaceae)," *Curr. Biol.*, vol. 34, no. 4, pp. 755–768.e4, 2024.

[22] M. S. Xavier et al., "Soft pneumatic actuators: A review of design, fabrication, modeling, sensing, control and applications," *IEEE Access*, vol. 10, pp. 59344–59385, 2022.

[23] D. Watson, L. A. Clark, and A. Tellegen, "Development and validation of brief measures of positive and negative affect: The PANAS scales," *J. Pers. Social Psychol.*, vol. 54, no. 6, 1988, Art. no. 1063.

[24] C. Bartneck, D. Kulić, E. Croft, and S. Zoghbi, "Measurement instruments for the anthropomorphism, animacy, likeability, perceived intelligence, and perceived safety of robots," *Int. J. Social Robot.*, vol. 1, no. 1, pp. 71–81, 2009.